

RESEARCH ARTICLE SUMMARY

NEUROSCIENCE

Striatal dopamine mediates hallucination-like perception in mice

K. Schmack*, M. Bosc, T. Ott, J. F. Sturgill, A. Kepecs*

INTRODUCTION: Psychotic disorders such as schizophrenia impose enormous human, social, and economic burdens. The prognosis of psychotic disorders has not substantially improved over the past decades because our understanding of the underlying neurobiology has remained stagnant. Indeed, the subjective nature of hallucinations, a defining symptom of psychosis, presents an enduring challenge for their rigorous study in humans and translation to preclinical animal models. Here, we developed a cross-species computational psychiatry approach to directly relate human and rodent behavior and used this approach to study the neural basis of hallucination-like perception in mice.

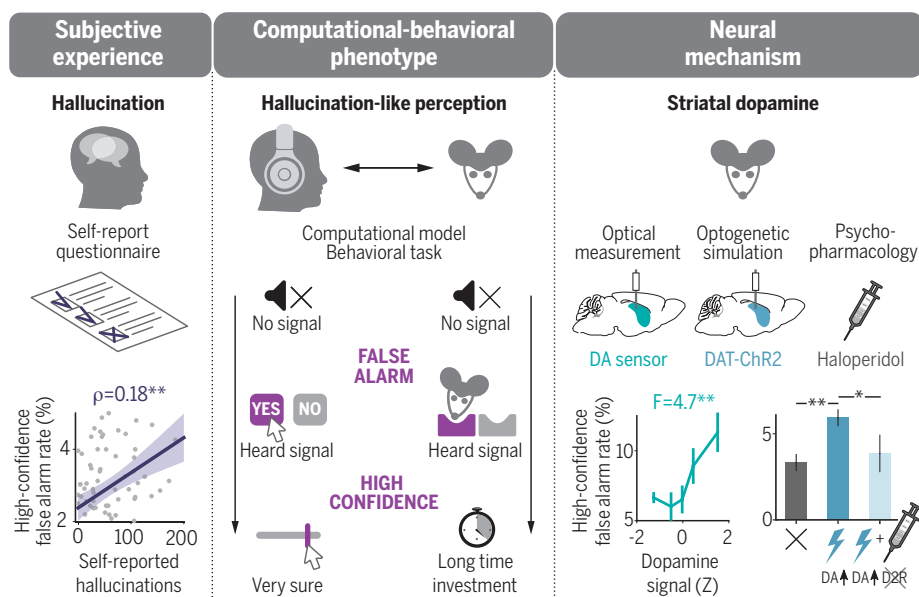
RATIONALE: Hallucinations are false percepts that are experienced with the same subjective confidence as “true” percepts. Similar false percepts can be quantitatively evaluated using a sensory detection task in which individuals report whether they heard a signal embedded in a background noise and indicate how confident

they are about their answer. Thus, we defined hallucination-like percepts as confident false alarms—that is, incorrect reports that a signal was present, which are reported with high confidence. We reasoned that such experimentally controlled hallucination-like percepts engage neural mechanisms shared with spontaneously experienced hallucinations in psychosis and can therefore serve as a translational model of psychotic symptoms. Because psychotic symptoms are thought to involve increased dopamine transmission in the striatum, we hypothesized that hallucination-like perception is mediated by increased striatal dopamine.

RESULTS: We set up analogous auditory detection tasks for humans and mice. Both humans and mice were presented with an auditory stimulus in which a tone signal was embedded in a noisy background on half of the trials. Humans pressed one of two buttons to report whether or not they heard a signal, whereas mice poked into one of two choice ports. Humans indicated how confident they were in

their report by positioning a cursor on a slider; mice expressed their confidence by investing variable time durations to earn a reward. In humans, hallucination-like percepts—high-confidence false alarms—were correlated with the tendency to experience spontaneous hallucinations, as quantified by a self-report questionnaire. In mice, hallucination-like percepts increased with two manipulations known to induce hallucinations in humans: administration of ketamine and the heightened expectation of hearing a signal. We then used genetically encoded dopamine sensors with fiber photometry to monitor dopamine dynamics in the striatum. We found that elevations in dopamine levels before stimulus onset predicted hallucination-like perception in both the ventral striatum and the tail of the striatum. We devised a computational model that explains the emergence of hallucination-like percepts as a consequence of faulty perceptual inference when prior expectations outweigh sensory evidence. Our model clarified how hallucination-like percepts can arise from fluctuations in two distinct types of expectations: reward expectations and perceptual expectations. In mice, dopamine fluctuations in the ventral striatum reflected reward expectations, whereas in the tail of the striatum they resembled perceptual expectations. We optogenetically boosted dopamine in the tail of the striatum and observed that increasing dopamine induced hallucination-like perception. This effect was rescued by the administration of haloperidol, an antipsychotic drug that blocks D2 dopamine receptors.

CONCLUSION: We established hallucination-like perception as a quantitative behavior in mice for modeling the subjective experience of a cardinal symptom of psychosis. We found that hallucination-like perception is mediated by dopamine elevations in the striatum and that this can be explained by encoding different kinds of expectations in distinct striatal subregions. These findings support the idea that hallucinations arise as faulty perceptual inferences due to elevated dopamine producing a bias in favor of prior expectations against current sensory evidence. Our results also yield circuit-level insights into the long-standing dopamine hypothesis of psychosis and provide a rigorous framework for dissecting the neural circuit mechanisms involved in hallucinations. We propose that this approach can guide the development of novel treatments for schizophrenia and other psychotic disorders. ■



Hallucination-like perception framework and striatal dopamine. In humans and mice, a computational-behavioral task models hallucinations as high-confidence false percepts. In humans, such hallucination-like percepts are correlated with self-reported hallucinations. In mice, hallucination-like percepts are mediated by striatal dopamine. Data are means \pm SEM. * $P < 0.05$, ** $P < 0.01$.

The list of author affiliations is available in the full article online.

*Corresponding author. Email: schmack@cshl.edu (K.S.);

akepecs@wustl.edu (A.K.)

Cite this article as K. Schmack et al., *Science* 372, eabf4740 (2021). DOI: 10.1126/science.abf4740

READ THE FULL ARTICLE AT
https://doi.org/10.1126/science.abf4740

RESEARCH ARTICLE

NEUROSCIENCE

Striatal dopamine mediates hallucination-like perception in mice

K. Schmack^{1*}, M. Bosc¹, T. Ott², J. F. Sturgill¹, A. Kepecs^{1,2*}

Hallucinations, a central symptom of psychotic disorders, are attributed to excessive dopamine in the brain. However, the neural circuit mechanisms by which dopamine produces hallucinations remain elusive, largely because hallucinations have been challenging to study in model organisms. We developed a task to quantify hallucination-like perception in mice. Hallucination-like percepts, defined as high-confidence false detections, increased after hallucination-related manipulations in mice and correlated with self-reported hallucinations in humans. Hallucination-like percepts were preceded by elevated striatal dopamine levels, could be induced by optogenetic stimulation of mesostriatal dopamine neurons, and could be reversed by the antipsychotic drug haloperidol. These findings reveal a causal role for dopamine-dependent striatal circuits in hallucination-like perception and open new avenues to develop circuit-based treatments for psychotic disorders.

Psychotic disorders such as schizophrenia rank among the main sources of global disease burden. Advances in the pharmacological treatment of psychotic disorders have been marginal because of our limited understanding of the disease mechanisms involved. Elevated dopamine is believed to induce psychotic symptoms because dopamine receptor blockers reduce psychotic symptoms (1), dopamine agonists can induce psychotic symptoms (2), and patients with psychosis show signs of increased dopamine transmission in the brain (3–5). However, the neural circuit mechanisms by which dopamine produces psychotic symptoms remain elusive. Studying psychotic disorders in animal models is challenging because the diagnosis relies on self-reported symptoms that can only be assessed in humans.

The core symptoms of psychosis, hallucinations and delusions, are subjective experiences not accessible to others. Because rodents cannot directly self-report their experiences, neuroscientists have relied on indirect behavioral measures of the disorder, such as drug-induced locomotion or pre-pulse inhibition of the startle reflex. These behavioral readouts have provided important neurobiological insights, but they typically do not predict human outcomes and their relationship with the phenomenology of psychotic symptoms is indirect (6). We addressed this challenge by developing a behavioral approach directly inspired by the phenomenology of hallucinations. Following the view that both subjective experience and observable behavior are the products of shared mental computations, we built on recent computational insights

into psychosis in humans (7, 8) and cognition in rodents (9, 10) to devise a behavioral paradigm for modeling hallucinations. Our approach is quantitative and applicable across species.

Hallucinations are false percepts that are experienced with the same subjective certainty or confidence as “true” percepts. We therefore operationalized hallucinations in a sensory detection task as false alarms (incorrect reports that a signal was present) that are experienced with high confidence. We reasoned that such experimentally controlled hallucination-like percepts (HALIPs) engage shared perceptual and neural processes as spontaneously experienced hallucinations in psychosis and can therefore serve as a translational model of psychotic symptoms.

Mice can report hallucination-like perceptions

We developed a psychometric auditory detection task with a postdecision confidence report (Fig. 1, A and B). Mice were presented with tone signals embedded in a white-noise background (40 dB SPL). We created perceptual ambiguity by presenting signals with graded levels of volume (35 to 65 dB SPL) that were interleaved across trials. Mice reported their perception by poking into one choice port if they perceived a signal and into another choice port if they did not perceive a signal. Correct choices (reporting signal at one port, “Hit”; reporting no-signal at the other port, “Correct reject”) led to a water reward delivered after a variable, unpredictable interval. The time duration that mice were willing to invest for a reward provides a quantitative measure of decision confidence (10–12). Mice were gradually trained to perform the task over several weeks (fig. S1).

After training was complete, mice performed the task well and their accuracy increased with the signal-to-noise ratio of the stimu-

lus, with a near-perfect performance for the loudest signal trials (Fig. 1C, psychometric function fit explained variance $R^2 = 0.99$). However, mice reported hearing signals on $16 \pm 4\%$ (mean \pm SD) of trials in which no signal was presented; hence, the task elicited a considerable fraction of false-alarm choices despite excellent overall performance.

Time investments made by mice were quantitatively explained by statistical decision confidence (13, 14) (fig. S2). Statistical decision confidence is defined as the probability of being correct for a given choice. We fit the observed psychometric choice behavior of mice to assess perceptual uncertainty, which enabled us to compute statistical confidence, the probability of being correct for each choice. Then, we used quantile normalization to transform these predicted probabilities into time investments (fig. S2, A to D). This method yielded a prediction about the statistically appropriate time investment without any free parameters (14). Time investments closely followed predicted statistical confidence: Time investments were calibrated to accuracy (Fig. 1D and fig. S3), were higher after correct choices than after error choices (Fig. 1E), and were predictive of psychometric choice behavior beyond external cues [all $T(7) > 2.65$, $P < 0.03$, paired t tests on all parameters of psychometric functions fit to choices with low or high invested time; Fig. 1F]. The predicted statistical confidence explained a substantial degree of variance in time investments [$R^2 = 0.84$, 0.43 to 0.95 (median, range across animals), all $P < 0.05$, product-moment correlation across stimulus-choice bins tested against 1000 permutations; Fig. 1G], demonstrating that mice allocated their time investment in a statistically appropriate manner. Time investments could thus be used as a behavioral readout of confidence.

Error rates were negligible on the loudest signal trials (Fig. 1C); hence, false alarms were unlikely to be caused by motor errors or inattentive lapses. False alarm rates were also not explained by spatial biases, because psychometric choice behavior was similar between groups of mice that used the right versus the left choice port to report a signal (fig. S3). False alarms were also unlikely to reflect simple reward-maximizing strategies. Correct choices were equally rewarded on signal and no-signal trials, and increased false alarm rates yielded decreased overall reward (fig. S4A). Furthermore, false alarms did not reflect lower task engagement, as false alarm rates were neither related to error rates on signal trials (fig. S4B) nor related to response times (fig. S4C). Finally, false alarms did not appear to be modulated by fatigue or satiety, because false alarm rates did not substantially change over the course of behavioral sessions (fig. S4D).

Time investments in false alarms were not readily explained by nonperceptual processes

¹Cold Spring Harbor Laboratory, Cold Spring Harbor, NY 11724, USA. ²Departments of Neuroscience and Psychiatry, Washington University School of Medicine, St. Louis, MO 63110, USA.
*Corresponding author. E-mail: schmack@cshl.edu (K.S.); akepecs@wustl.edu (A.K.)

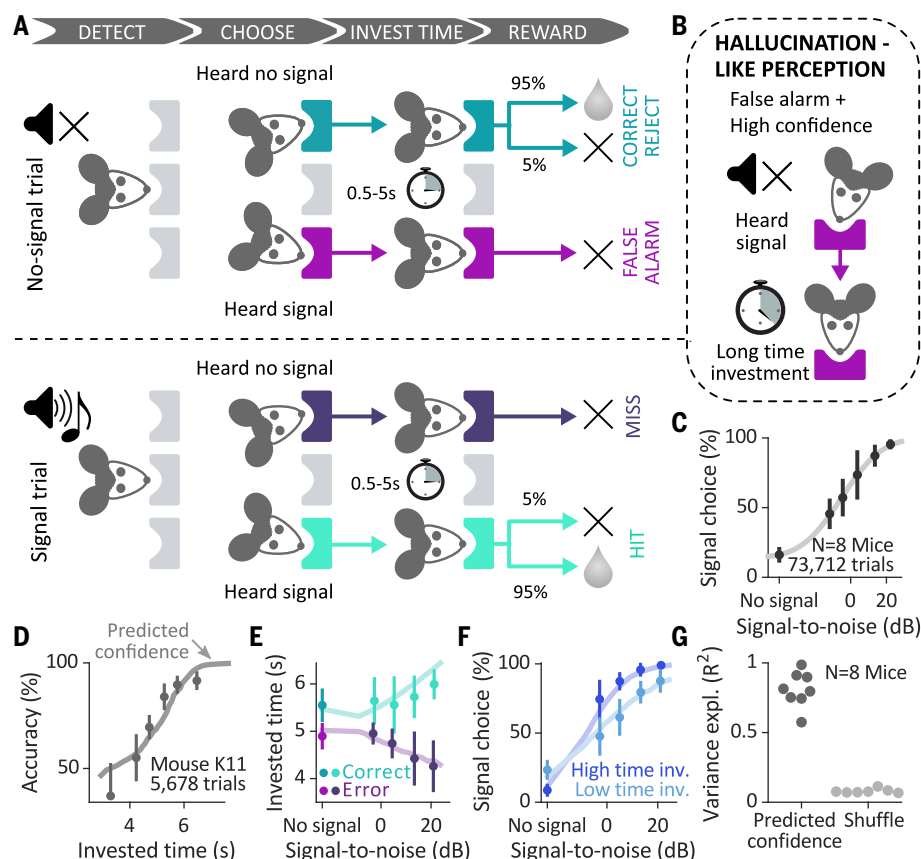


Fig. 1. Mice can report hallucination-like perception. (A) Schematic of behavioral task to quantify hallucination-like perception. (B) Operational definition of hallucination-like perception. (C) Choice behavior follows a psychometric function. Signal choice percentage (mean \pm SD across mice) is fit by a psychometric function (gray line). The leftmost data point indicates that mice exhibited false alarms. (D to F) Time investment behavior follows statistical decision confidence in an example mouse. Behavior (mean \pm SD across sessions) parallels predicted confidence from a statistical definition of confidence (light-shaded lines). Note that predicted confidence does not represent a fit to the time investments but is computed from an individual's psychometric choice behavior (14). Data are separated for correct and error trials (E) and for above-median and below-median time investments (F). Data are corrected for between-session variance by subtracting the session mean and adding the grand mean. (G) Time investment behavior follows statistical decision confidence in all mice. Explained variance in time investment behavior is higher for confidence predicted from a statistical definition of confidence (left) than for shuffled control (right).

unrelated to confidence. They were part of the overall pattern of time investments whose durations can be explained by a statistically appropriate use of perceptual confidence (Fig. 1, D to G). The distribution of time investments on false alarms showed trial-to-trial variability and substantial overlap with the distribution of time investments on hits (fig. S4, E to L). This indicates that the false alarms with the largest time investments were perceived with comparable confidence as “true” signals, and therefore likely reflected high-confidence faulty percepts (i.e., HALIPs).

Hallucination-like perception is increased by hallucination-related manipulations in mice

We tested whether two manipulations related to symptomatic hallucinations in humans alter

hallucination-like perception in mice. First, humans with symptomatic hallucinations are more susceptible to the influence of expectations during perceptual tasks (15). Therefore, we tested whether increasing expectations of hearing a signal would induce more HALIPs in mice. We varied signal expectations by changing the proportion of signal versus no-signal trials across blocks of 200 trials within each session (signal/no-signal ratio: 0.3:0.7, 0.5:0.5, or 0.7:0.3). In blocks with higher signal expectations, both false alarm rate and time investment-based confidence in false alarms were increased [$F(2, 14) = 20.5$, $P < 0.001$, and $F(2, 14) = 11.6$, $P < 0.001$, respectively, repeated-measures analysis of variance (ANOVA) across mice; Fig. 2, A and B]. In line with this, signal expectations increased high-confidence

false alarms [$F(2, 14) = 18.4$, $P < 0.001$; Fig. 2C], with somewhat weaker effects on low-confidence false alarms [$F(2, 14) = 12.2$, $P < 0.001$; data S1]. Increasing signal expectations did not degrade perceptual performance in general; rather, it biased perception toward perceiving more signals and thereby produced more false alarms (Fig. 2D). Moreover, time investments remained calibrated to accuracy for all signal expectations (Fig. 2, E to G), and the slope of the calibration curve and the degree of variance explained by statistical decision confidence did not differ across different signal proportions [$F(2, 14) = 1.2$, $P = 0.34$, and $F(2, 14) = 1.1$, $P = 0.36$, respectively; Fig. 2H].

We next tested whether ketamine, a drug known to induce psychotic experiences including perceptual distortions in humans (16), also induces HALIPs in mice. Prior to behavioral testing, mice received sub-anesthetic doses of vehicle (0.9% saline) or ketamine (intraperitoneal, 30 mg/kg) that produced stereotypical circling behavior for a few minutes before beginning the task. Ketamine increased both the false alarm rate and time investment-based confidence in false alarms [$F(1, 7) = 10.0$, $P = 0.02$, and $F(1, 7) = 9.6$, $P = 0.02$, respectively; repeated-measures ANOVA across mice; Fig. 2, I and J]. In line with this, ketamine increased high-confidence false alarms [$F(1, 7) = 22.1$, $P = 0.002$; Fig. 2K] but not low-confidence false alarms [$F(1, 7) = 2.0$, $P = 0.20$; data S1]. The effects of ketamine rapidly diminished over the first hour after drug administration, as expected from the relatively short half-life of ketamine, ~45 min (Fig. 2M and fig. S5). Crucially, ketamine did not degrade perceptual performance, but instead biased perception toward higher false alarm rates (Fig. 2L). Moreover, time investment-based confidence remained calibrated to statistical confidence regardless of drug administration (Fig. 2, N and O), and the slope of the calibration curve and the degree of variance explained by statistical confidence were not different between the drug conditions [$F(1, 7) = 0.0$, $P = 0.9$, and $F(2, 14) = 0.1$, $P = 0.74$, respectively; Fig. 2P].

Hallucination-like perception is correlated with self-reported proneness to hallucinations

To determine how our behavioral task is related to the subjective experience of hallucinations, we correlated objectively quantified HALIPs with self-reported proneness to hallucinations in humans. We created a computerized, online version of our auditory detection task that allowed us to quantify HALIPs in human participants recruited on a crowdsourcing website (Fig. 3A, $n = 220$) (14). As in the mouse task, in the human task we presented signals of varying volume embedded in noise. Human participants reported whether or not they heard a signal by pressing a key and explicitly reported their confidence ratings by positioning

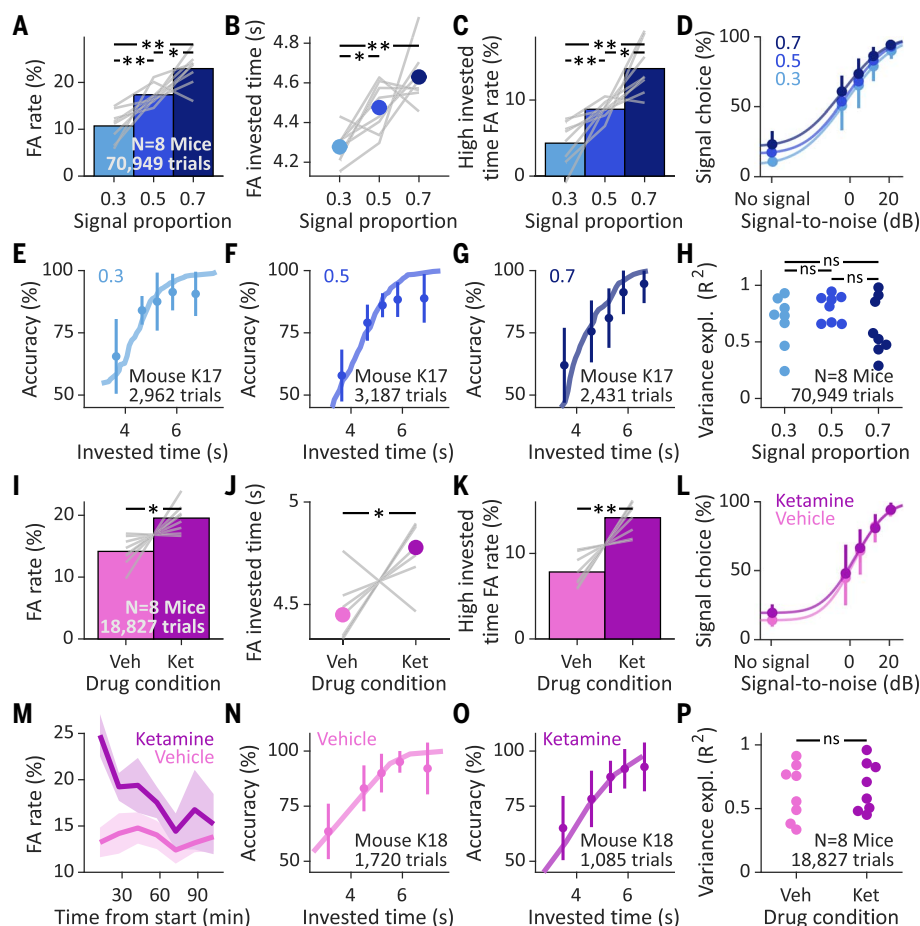


Fig. 2. Hallucination-like perceptions are increased by hallucination-related manipulations in mice.

(A to C) Expectations of hearing a signal increase hallucination-like perceptions. Signal expectations are experimentally manipulated by changing the proportion of signal trials. Increasing signal proportion increases false alarm (FA) rate (A) and time investment–based confidence in false alarms (B) as well as the rate of false alarms with high confidence, as defined by above-median time investments (C). Bars and dots are group means; gray lines are individual subjects. Data are corrected for between-subjects variance by subtracting the subjects' grand mean and adding the group grand mean. (D) Psychometric choice behavior shows that signal expectations bias perception toward perceiving more signals, thereby increasing false alarm rates (leftmost data points). (E to G) Time investment behavior follows statistical confidence independent of signal expectation. Time investments are calibrated to accuracy (mean \pm SD across sessions) and reflect predicted statistical confidence (shaded lines) for low (E), intermediate (F), and high (G) signal proportion. Note that predicted confidence does not represent fits to the time investments, but is computed from its respective psychometric function. (H) Predicted statistical confidence explains variance in time investment–based confidence to similar degrees across different signal expectations. (I to K) Ketamine induces hallucination-like perceptions. Relative to saline (Veh), ketamine (Ket; 30 mg/kg) increases false alarm rate (I), time investment–based confidence in false alarms (J), and the rate of high-confidence false alarms, as defined by the above median time investments (K). (L) Psychometric choice behavior after ketamine is biased toward higher false alarm rates (leftmost data point) while not disrupting perceptual performance on signal trials (data points at right). (M) The effects of ketamine decrease over time, in line with the substance's half-life of ~ 45 min (see also fig. S5). (N and O) Time investment behavior follows statistical confidence similarly for vehicle (N) and ketamine (O). (P) Statistical decision confidence explains variance in time investment–based confidence to similar degrees after vehicle and ketamine. * $P < 0.05$, ** $P < 0.01$ (post hoc tests in repeated-measures ANOVA across subjects); ns, not significant.

a slider. The performance of human participants was similar to what we had observed in mice: **Perceptual choices followed a psychometric function with a substantial false alarm rate of $7 \pm 4.5\%$** (mean \pm SD across participants) (Fig. 3B), and confidence reports

reflected statistical decision confidence [$R^2 = 0.61$, 0.29 to 0.80 (median, interquartile distance across participants), $P < 0.05/0.1/0.2$ in 66/75/85% of participants, product-moment correlation across stimulus bins tested against 1000 permutations; Fig. 3, C to F].

Our measure of HALIPs, high-confidence false alarms, was correlated with self-reported proneness to hallucinations. To assess this, we administered self-report questionnaires that are designed to evaluate psychiatric symptoms in the general population (17, 18). **Hallucination proneness scores in our nonclinical sample were spread across the entire range**, corroborating previous studies that psychotic symptoms, similar to other dimensions of psychopathology, **present as a continuous phenotype and are not always associated with a clinical diagnosis** (19). The degree of self-reported hallucinations was positively correlated to both false alarm rate and false alarm confidence ($\rho = 0.17$, $P = 0.01$, and $\rho = 0.18$, $P = 0.01$, respectively; Spearman rank correlation; Fig. 3, G and H), similar to previous findings in nonclinical and clinical samples (7). In line with this, self-reported hallucinations were positively correlated to high-confidence false alarms ($\rho = 0.18$, $P = 0.01$; Fig. 3I). By contrast, miss rates on signal trials were not correlated to questionnaire scores ($\rho = -0.04$, $P = 0.56$), indicating that self-reported hallucinations were not associated with generally poor performance.

Other psychopathology dimensions such as somatization and anxiety were also correlated with hallucinations ($\rho = 0.55$ to 0.68), as well as with each other ($\rho = 0.55$ to 0.93), confirming the widely recognized overlap between different psychopathological categories. Consequently, psychopathology dimensions other than hallucinations also showed varying degrees of correlation to HALIPs ($\rho = 0.02$ to 0.18 ; Fig. 3J). **To identify the independent contribution of symptom dimensions, we performed a stepwise multiple regression analysis.** The hallucination dimension alone accounted best for both false alarm rates and confidence [stepwise regression on rank-transformed data, $F(1, 218) = 6.88$, $P = 0.01$, and $F(1, 218) = 7.49$, $P = 0.007$], indicating that HALIPs were most strongly and specifically related to hallucinations.

Belief-updating model accounts for hallucination-like perception

We next devised a computational model that explains the emergence of HALIPs as quantifiable moment-to-moment estimates of beliefs and provides a link to the underlying neural processes. When faced with an ambiguous stimulus, such as a faintly uttered word in a noisy room, our prior expectations help to interpret it. **Hallucination-like percepts might occur as faulty perceptual inferences due to biased expectations, in line with Bayesian theories of hallucination** (15). To explore this idea, we built a simple computational model for the auditory detection task that combines current sensory evidence with prior expectations to produce choices and adjusts expectations based on outcomes (Fig. 4A) (14). Expectations are modeled as a probabilistic

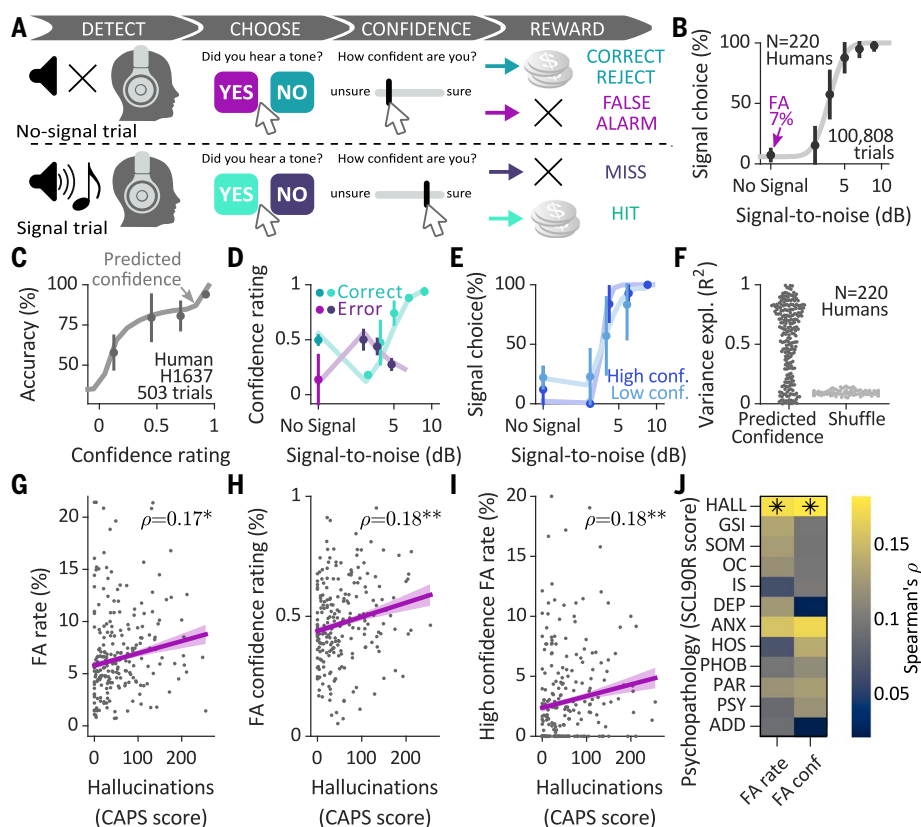


Fig. 3. Self-reported proneness to hallucination relates to hallucination-like perception. (A) Schematics of human online task to quantify hallucination-like perception. (B) Choice behavior follows psychometric function. Signal choice percentage (mean \pm SD across participants) is fit by a psychometric function (gray line). The leftmost data point indicates that human participants exhibited false alarms at a rate of 7%. (C to E) Confidence ratings follow statistical decision confidence for an example participant. Data points (mean \pm SD across sessions) follow statistical decision confidence as predicted from choice behavior (light-shaded lines). Data are separated for correct and error trials (D) and above-median and below-median confidence trials (E). Note that predicted confidence does not represent fits to the time investments, but is computed from an individual's psychometric choice behavior. (F) Confidence ratings follow statistical decision confidence in a majority of the cohort. Explained variance in confidence ratings is higher for confidence predicted from a statistical definition of confidence (left) than for shuffled control (right). Dots represent single participants. (G to I) Self-reported proneness to hallucination correlates with hallucination-like perception but not with perceptual performance in general. Graphs show relations between sum scores from the Cardiff Anomalous Perception Scale [CAPS score (17)] and false alarm rate (G), false alarm confidence ratings (H), and high-confidence false alarm rate (I). High confidence was defined as above-median confidence. Dots represent single participants; a line shows the fit (\pm SE) of a robust regression model. * $P < 0.05$, ** $P < 0.01$ (Spearman's rank correlation). (J) Hallucination-like perception is more strongly related to self-reported proneness to hallucination than to other psychopathological dimensions. The heatmap shows relations between Pearson Clinical Symptom Checklist 90-R scores and false alarm rate (left) and false alarm confidence ratings (right). Asterisks denote dimensions that were identified to predict false alarm rate and confidence by a stepwise regression on the rank-transformed data. HALL, hallucination proneness; GSI, Global Severity Index; SOM, somatization; OC, obsessive-compulsive; IS, interpersonal sensitivity; DEP, depression; ANX, anxiety; HOS, hostility; PHOB, phobic anxiety; PAR, paranoia; PSY, psychoticism; ADD, additional items.

prior belief, μ_P . In each trial, this prior belief is combined with the current sensory evidence (Bayesian inference), and the resulting posterior belief gives rise to both a perceptual decision and confidence about the decision. Once feedback is received about the decision outcome (signal/no-signal), a perceptual prediction error δ (Bayesian surprise) is computed as the difference between the actual occurrence of a signal

and the confidence in the occurrence of a signal. This perceptual prediction error δ then updates the prior belief μ_P with a fixed learning rate α .

Using this model, we simulated the detection task with trial sequences from our experiments. Simulated model behavior closely mirrored the behavior observed in mice and humans: Perceptual choices followed a psychometric function with a substantial false alarm rate, and

confidence behaved like statistical decision confidence (Fig. 4, B and C; compare with Fig. 1, C and E, and Fig. 3, B and D). The model also explains how increasing signal expectation produces HALIPs (more false alarms with higher confidence) (Fig. 4, E and F; compare with Fig. 2, A and B) as a consequence of learning, as the updated prior μ_P tracks changing signal proportions (Fig. 4D).

A key prediction of belief-updating models is that perception should systematically fluctuate from trial to trial based on previous outcomes (20). Consistent with this prediction after correct choices, mice tended to bias their perceptual choices toward the previous choice [$F(1, 20) = 43.4$, $P < 0.001$, repeated-measures ANOVA across mice; Fig. 4G], particularly when the previous choice was difficult and hence decision confidence was low (Fig. 4I). Our model produces the same pattern of trial-by-trial choice updates: The prior expectation μ_P shifts toward the correct choice, thereby increasing the probability of repeating this choice in the next trial. Moreover, the size of the shift of μ_P depends on the absolute size of the prediction error δ . Because the absolute size of δ is larger when decision confidence is low, the probability of repeating a choice in the next trial is higher after more difficult, low-confidence, choices. Indeed, simulated behavior exhibited trial-by-trial choice updates (Fig. 4H) that depended on difficulty (Fig. 4J), in a manner very similar to the behavior observed in mice (Fig. 4, G and I).

The belief-updating model makes specific predictions about how HALIPs arise from fluctuations in two distinct types of expectations: reward expectations and perceptual expectations (Fig. 4K) (14). The impact of perceptual expectations can be quantified by the signed value of the prior, or μ_P . Increasing μ_P will produce higher signal expectations and bias choice behavior toward increased signal choices and their confidence for both signal and no-signal trials. Thus, high perceptual expectations will produce overconfident false alarms (i.e., HALIPs) but will also lead to more hits (Fig. 4K, right). Although the model does not explicitly consider reward expectations, high expectations of either a signal or a no-signal stimulus indicate high reward expectations because both correct signal detections and correct no-signal rejections are rewarded. Thus, reward expectations can be captured by the absolute distance of the prior from the average stimulus, $|\mu_P|$. When reward expectations $|\mu_P|$ are high, the posterior will be far from the average stimulus. Consequently, error choices and their confidence increase for both signal and no-signal trials, producing more overconfident false alarms (i.e., HALIPs) while also leading to more misses (Fig. 4K, center). We hypothesized that striatal dopaminergic activity encodes either of these decision variables underlying HALIPs.

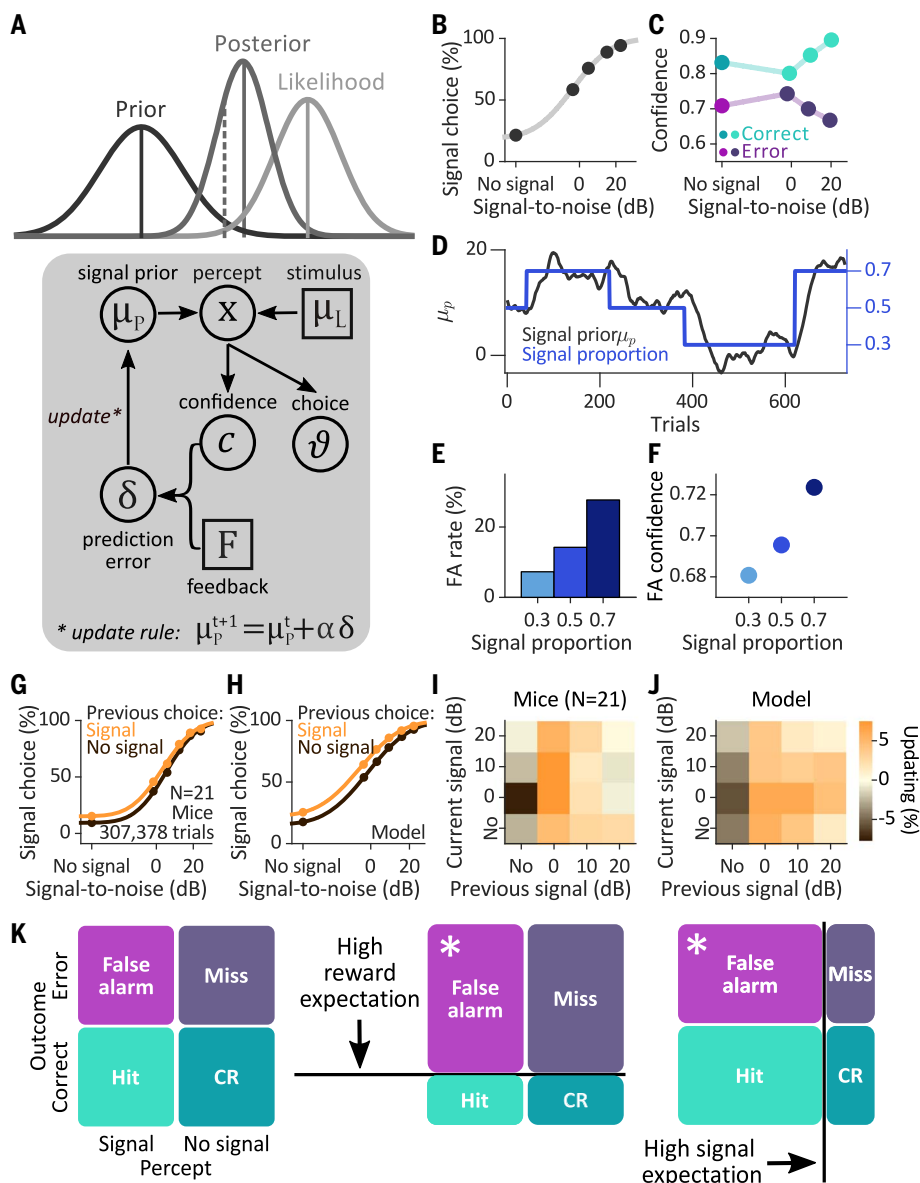


Fig. 4. Belief-updating model accounts for hallucination-like perception. (A) Schematic of belief-updating model. Confidence and choice are derived from Bayesian inference (top); learning is guided by prediction error–based updating (bottom). (B and C) Simulated choice (B) and confidence (C) behavior closely resemble behavior observed in mice and humans (compare Figs. 1 and 3). (D) Simulated signal prior tracks experimentally induced signal expectations. (E and F) Simulated effect of signal expectations on hallucination-like perceptions. Both simulated false alarm rate (E) and simulated false alarm confidence (F) recapitulate observed behavior (compare Fig. 2). (G and H) The model reproduces trial-by-trial updating of perceptual choices. After correct choices, mice tend to shift their perceptual choice toward the previous perceptual choice [(G), $P < 0.001$, repeated-measures ANOVA across mice]. Behavior simulated with the belief-updating model reproduces this effect (H). (I and J) The model reproduces stimulus dependence of trial-by-trial choice updating. Choice updating (i.e., the size of psychometric curve shift relative to the average psychometric curve) is a function of signal-to-noise ratio in the previously correct trial and current trial. Positive numbers refer to a bias toward signal choices. Observed mouse behavior (I) is mirrored by simulated model behavior (J). (K) Model predictions for how expectations lead to hallucination-like perception. Left: Choices and confidence can be grouped according to outcome and percept. Center: High reward expectations lead to more error choices and higher confidence in errors, thereby producing overconfidence in false alarms. Right: Perceptual expectations lead to more signal choices and higher confidence in signal choices, thereby producing overconfidence in false alarms. Rectangle area sizes symbolize choice proportion and confidence. Asterisks denote hallucination-like percepts. CR, correct rejection.

Elevated dopamine in ventral striatum and tail of striatum precedes hallucination-like perception

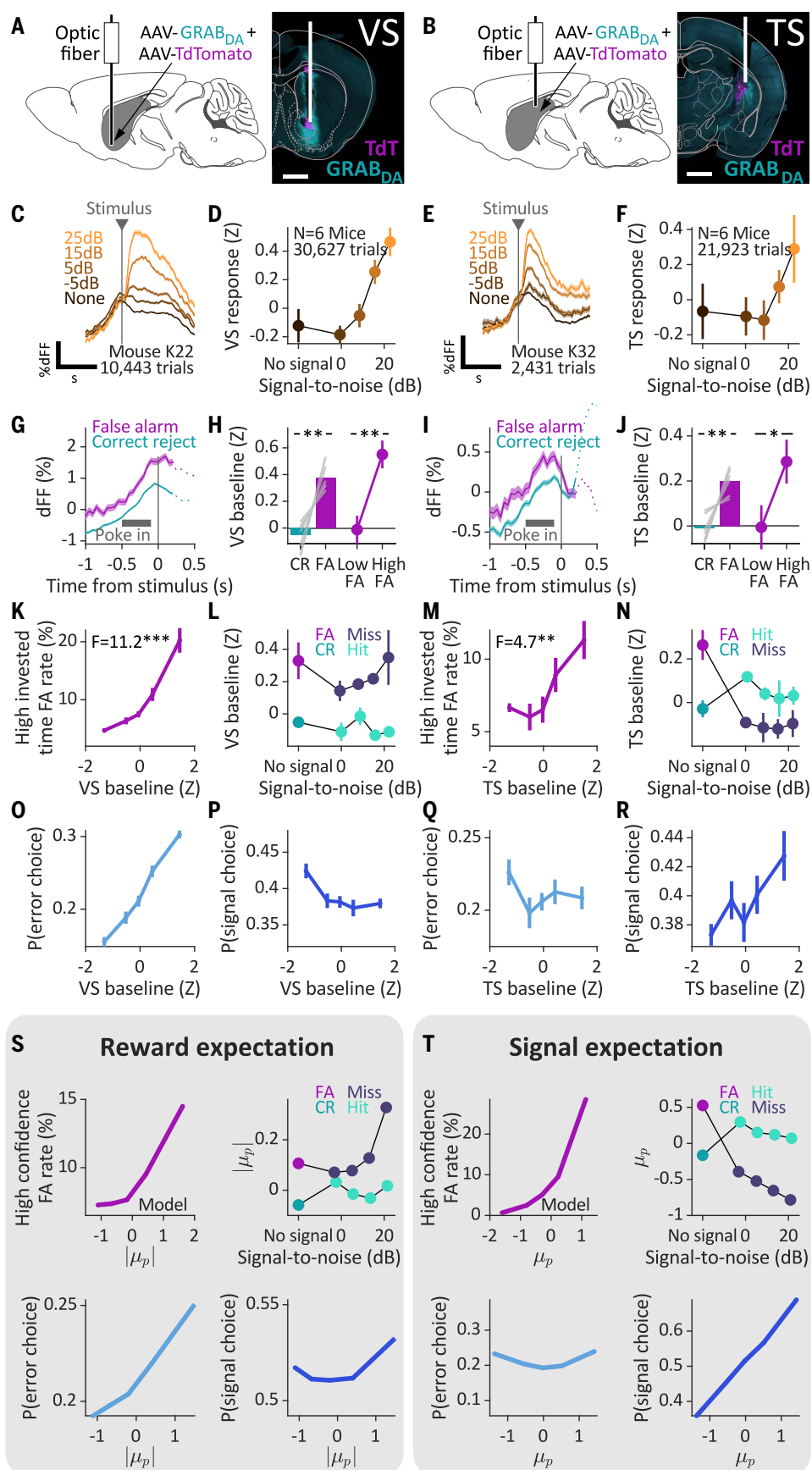
We tested whether and how dopamine dynamics are predictive of HALIPs in mice. On the basis of our model predictions that dopamine might lead to HALIPs through either reward expectations or perceptual expectations, we selected two striatal regions: the ventral striatum (VS), known for its role in reward processing (21), and the dorsal tail of the striatum (TS), which has been implicated in perceptual processing (22, 23). To measure dopamine, we virally expressed a dopamine fluorescence sensor, GRAB_{DA} (24), and used fiber photometry in behaving mice (Fig. 5, A and B) (14). We observed phasic dopamine responses to reward outcomes (fig. S7) and to stimulus delivery (Fig. 5, C and E) in both TS and VS. Stimulus responses were smallest on no-signal trials and increased with stimulus strength on signal trials (Fig. 5, D and F), consistent with previous work showing scaling of phasic dopamine responses with external stimulus intensity (23).

Surprisingly, tonic dopamine levels prior to stimulus delivery were predictive of upcoming HALIPs in both VS and TS. Because HALIPs, by definition, occur on no-signal trials, we first focused our analyses on false alarms and correct rejections. Dopamine levels were higher before false alarms than before correct rejections throughout the pre-stimulus period (Fig. 5, G and I, and fig. S8, A and B), and this observation was consistent across animals [VS, $T(5) = 5.50$, $P = 0.003$; TS, $T(5) = 4.32$, $P = 0.008$; paired t tests across animals; Fig. 5, H and J]. Moreover, pre-stimulus dopamine was elevated before high compared to low time investment-based confidence conditions in false alarm trials [VS, $T(5) = 5.29$, $P = 0.003$; TS, $T(5) = 2.92$, $P = 0.03$; Fig. 5, H and J], with weaker or no effects on time investment-based confidence in other trial types (fig. S10, E to L). Moreover, dopamine levels before stimulus delivery predicted the rate of high-confidence false alarms in a graded manner [VS, $F(4, 20) = 11.2$, $P < 0.001$; TS, $F(4, 20) = 4.7$, $P = 0.008$; repeated-measures ANOVAs across animals; Fig. 5, K and M].

Our model predicts that the link between dopamine and HALIPs might be due to either reward expectations or perceptual expectations with differing consequences during signal trials (Fig. 4K). To test these predictions, we extended our analyses to signal trials, revealing a dissociation between striatal subregions. VS dopamine was higher before error than before correct signal trials (i.e., misses versus hits) [$T(5) = -7.53$, $P < 0.001$; Fig. 5L], whereas TS dopamine showed the opposite pattern [$T(5) = 2.16$, $P = 0.08$; Fig. 5N]. We next considered how well these differences could predict either the probability of reporting that a signal was

Fig. 5. Increased baseline dopamine in ventral striatum and tail of striatum precedes hallucination-like perception.

(A and B) Photometry approach and fiber placement for measuring dopamine in ventral striatum (VS) and tail of striatum (TS) while mice performed the behavioral task for measuring hallucination-like perception (see Fig. 1A). GRAB_{DA} dopamine sensor was used to measure dopamine; tdTomato was used to correct for movement artifacts. (C to F) Phasic dopamine responses to stimulus delivery in VS [(C) and (D)] and TS [(E) and (F)]. Example dopamine signal time series [(C) and (E)] and response amplitudes [(D) and (F)] show increasing responses with increasing stimulus signal-to-noise ratio. Dopamine signal traces are normalized with respect to a moving time window and are corrected for movement (dFF). Response amplitude (mean \pm SEM across mice) is the difference between maximum signal and time-point zero signal and is z-scored within subject. (G to R) Tonic baseline dopamine is increased prior to hallucination-like perceptions in both VS (left columns) and TS (right columns), but for different reasons. Example dopamine time series [(G) and (I)] show tonic increase prior to false alarms (FA) versus correct rejection (CR). In both regions, baseline dopamine is increased prior to FA versus CR [(H) and (J), bar plots] and prior to FA with high versus low time investment-based confidence [(H) and (J), dot plots]. Accordingly, in both regions, baseline DA is tuned to upcoming hallucination-like perceptions (i.e., the rate of high-confidence false alarm rates) [(K) and (M)]. However, in VS, baseline DA is increased prior to error choices (L) and tuned to error choice probability [(O) and (P)], thereby accounting for hallucination-like perceptions. In TS, baseline DA is increased prior to signal choices (N) and tuned to signal choice probability [(Q) and (R)], thereby accounting for hallucination-like perceptions. Baseline dopamine is the signal integrated over a 0.5-s interval before the trial initiation poke and is z-scored within subject. (S and T) Prior expectations from belief-updating model match dopamine signals in VS and TS. Reward expectations, quantified by $|\mu_p|$, recapitulate signals in VS (S); signal expectations, quantified by μ_p , resemble signals in TS (T). * $P < 0.05$, ** $P < 0.01$, *** $P < 0.001$ (main effects from repeated-measures ANOVA across subjects). High and low confidence are defined by a median split on the time investments. Data are means \pm SEM across subjects. Gray lines represent single subjects.



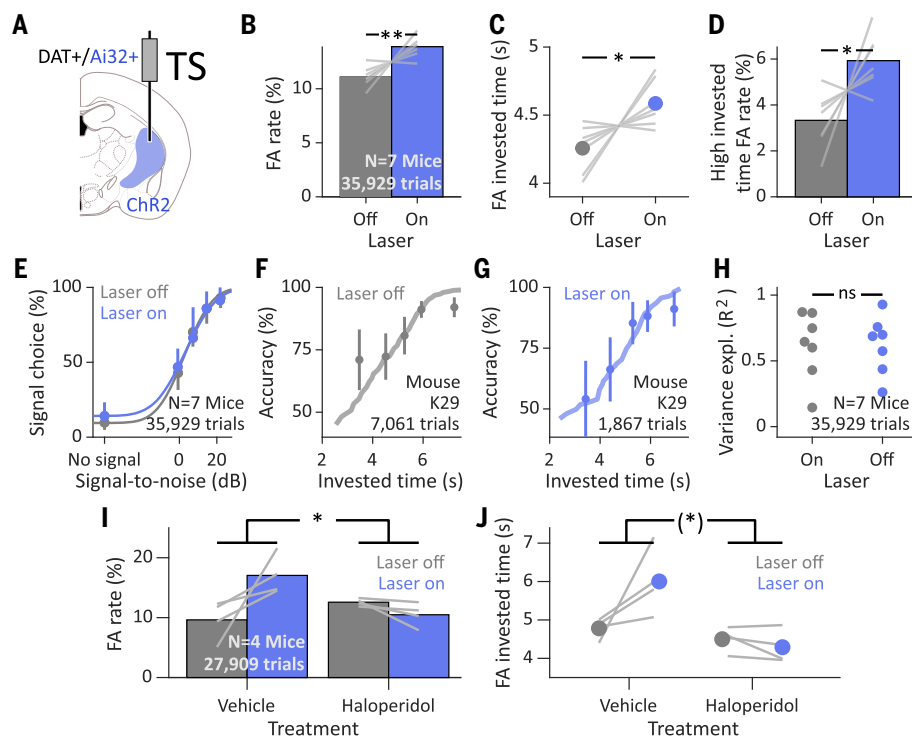


Fig. 6. Dopamine in tail of striatum is causal for hallucination-like perceptions. (A) Fiber placement for optical stimulation of dopaminergic axons in tail of striatum. (B to D) Optogenetic stimulation increases false alarm rate (B), time investment-based false alarm confidence (C), and the rate of high-confidence false alarms as defined by above-median time investments (D). Bar plots are means across subjects; gray lines are single subjects. (E) Optogenetic stimulation increases false alarm rate without a nonspecific disruption of psychometric choice behavior or changing miss rate on signal trials. Data are means \pm SD across subjects [$F(1, 6) < 0.1$, $P = 0.90$]. (F and G) Optogenetic stimulation does not affect overall time investment-based confidence report. Time investments (mean \pm SD across sessions) follow statistical decision confidence (line) both without stimulation (F) and during stimulation (G). Note that predicted confidence does not represent fits to the time investments, but is computed from the individual's psychometric choice behavior in the respective experimental condition. (H) Across-animals variance explained by statistical confidence was not different between off- and on-stimulation trials [$F(1, 6) < 0.1$, $P = 0.94$]. (I and J) Haloperidol rescue of optogenetic effect on false alarm rate (I) and false alarm confidence (J). (*) $P < 0.1$, * $P < 0.05$, ** $P < 0.01$, post hoc test [(B) to (D)] or interaction effect [(I) and (J)] repeated-measures ANOVA across subjects. In group plots, data are corrected for between-subjects variance by subtracting the subjects' grand mean and adding the group grand mean.

present (hit and false alarm) or the probability of making an error (false alarm and miss).

Dopamine levels prior to stimulus presentation in VS predicted upcoming error probability rather than upcoming signal choice probability (Fig. 5, O and P). In contrast, TS dopamine was more predictive of upcoming signal choice probability than of upcoming error probability (Fig. 5, Q and R). In line with this, VS dopamine was positively related to upcoming false alarm probability and negatively related to upcoming hit probability, whereas TS dopamine was positively related to both upcoming false alarm and hit probability, indicating that the observed dissociation between VS and TS was present on both no-signal and signal trials (fig. S10, A to D). This dichotomy in patterns of tonic DA was present

for both ipsilateral and contralateral movements for signal choice reports; this finding suggests that the observed dissociation between VS and TS could not be explained by differential involvement in movement preparation (fig. S9).

These two patterns of dopamine responses matched our two alternative model predictions for how dopamine relates to HALIPs (Fig. 4K). Reward expectations were proportional to $|\mu_P|$, a variable that closely resembled baseline dopamine in VS, whereas perceptual expectations, quantified by μ_P , behaved like baseline dopamine in TS. On no-signal trials, both reward and signal expectations accounted for HALIPs, because both $|\mu_P|$ and μ_P were higher before false alarms than before correct rejections (Fig. 5, S and T, top right), and also predicted the rate of high-confidence false

alarms (Fig. 5, S and T, top left). On signal trials, however, $|\mu_P|$ was higher before error choices than before correct choices (i.e., misses versus hits) and therefore specifically predicted error probability (Fig. 5S), paralleling VS dopamine. In contrast, μ_P was higher before correct choices than before error choices (i.e., hits versus misses) and consequently predicted signal choice probability (Fig. 5T), paralleling TS dopamine.

Thus, elevated levels of dopamine precede HALIPs in both striatal subregions examined, but for different reasons. VS tonic dopamine is predictive of future outcomes, consistent with the encoding of reward expectations. Increased reward expectations in turn produce higher confidence error choices, thereby leading to HALIPs. TS tonic dopamine, in contrast, is predictive of future signal perception, consistent with the encoding of perceptual expectations. Increased perceptual expectations bias perceptual detection toward signals to increase signal choices and confidence, thereby producing HALIPs.

Elevated dopamine in tail of striatum produces hallucination-like perception

We next investigated whether optogenetically boosting dopamine levels in the striatum specifically increases HALIPs. To ensure sufficient trial numbers across different optogenetic and pharmacological conditions, we concentrated on one striatal subregion. We selected the tail of the striatum because our photometry results pointed to a link between TS dopamine and HALIPs due to perceptual rather than reward-related processes. Transgenic mice expressing channelrhodopsin-2 in dopamine neurons (DAT-Ai32) performed the detection task while we used tonic laser stimulation to stimulate axonal dopamine release in TS across blocks of trials (Fig. 6A, 2 Hz, 0.5 mW, continuous stimulation over 50 trials interleaved with no stimulation over 100 to 200 trials). Both false alarm rate and confidence-guided time investment in false alarms were increased on optogenetic stimulation trials as compared to no-stimulation trials [$F(1, 6) = 15.1$, $P = 0.008$, and $F(1, 6) = 6.6$, $P = 0.042$; repeated-measures ANOVAs across mice; Fig. 6, B and C]. Optogenetic stimulation particularly increased high-confidence false alarms [$F(1, 6) = 7.9$, $P = 0.03$; Fig. 6D], with weaker effects on low-confidence false alarms [$F(1, 6) = 5.8$, $P = 0.05$; data S1]. Optogenetic stimulation did not degrade perceptual performance in general, but rather increased false alarms without affecting overall misses [$F(1, 6) < 0.1$, $P = 0.90$; Fig. 6E]. Optogenetic stimulation also did not disrupt time investment-based confidence behavior in general, as time investments were calibrated to accuracy during both off- and on-stimulation trials and predicted statistical decision confidence (Fig. 6, F and G), and the slope of the calibration curves and degree of variance explained by statistical

confidence was not different between off- and on-stimulation trials [$F(1, 6) < 0.1$, $P = 0.85$, and $F(1, 6) < 0.1$, $P = 0.94$, respectively; Fig. 6H].

An antipsychotic drug, the dopamine receptor D2 antagonist haloperidol, rescued the optogenetically induced effects on HALIPs. Optogenetically induced dopamine increased false alarm rate and false alarm confidence after treatment with vehicle, and this increase was reversed after treatment with haloperidol (0.15 to 0.25 mg/kg) [optogenetic stimulation \times treatment interactions, $F(1, 3) = 11.2$, $P = 0.04$, and $F(1, 3) = 6.66$, $P = 0.08$, for false alarm rate and confidence, respectively; Fig. 6, I and J].

Discussion

We established hallucination-like percepts as a quantitative behavioral readout of hallucinations in mice. HALIPs, high-confidence false percepts, increased after hallucination-related manipulations in mice and correlated with self-reported hallucinations in humans. HALIPs were preceded by increased tonic levels of dopamine in the striatum, which can be explained by the encoding of reward and perceptual expectations in the ventral striatum and the tail of the striatum, respectively. HALIPs could be induced by optogenetic stimulation of dopamine in the tail of the striatum and were reversed by the antipsychotic haloperidol. Taken together, our behavioral readout of hallucinations opens a new avenue toward a mechanistic, circuit-level explanation for how excessive dopamine produces hallucinations, a cardinal symptom of psychotic disorders.

Animal models that fully recapitulate the diagnostic criteria for psychotic disorders are impossible because animals cannot describe their subjective experiences. Therefore, previous studies have focused on “endophenotypes,” indirect markers that are affected in schizophrenia patients. Such endophenotypes encompass innate behaviors, such as a disinhibited startle reflex after a pre-pulse or drug-induced locomotion, and neurophysiological markers, such as reduced neural responses to oddball stimuli or diminished prefrontal-hippocampal synchrony (25, 26).

We used a computational approach to develop a quantitative behavioral readout of a highly subjective yet defining symptom of psychosis, hallucinations. We believe our approach of directly modeling a defining symptom of psychotic disorders presents several advantages over previous endophenotype approaches. First, the direct phenomenological connection reduces the danger of probing auxiliary disease mechanisms: Overconfident false alarms in a psychometric auditory detection likely engage the same perceptual and neural processes that are involved in spontaneous hallucinations. Second, the behavioral task used can be easily translated back and forth between mice and humans. Such seamless translation enables

iterative improvements of our task—for instance, based on its prognostic value in patients. Third, HALIPs are psychometrically defined along several dimensions on a per-decision basis, providing a level of resolution that is well suited for neural circuit studies. This is exemplified by our observations about dopamine: Although false alarm rates and confidence demonstrated a role for dopamine in HALIPs, psychometric choice behavior on signal trials differentiated between alternative underlying processes in different subregions of the striatum. Taken together, HALIPs are a promising model for mechanistic studies of psychosis.

Our results provide circuit-level evidence for the dopamine hypothesis of schizophrenia. Excessive dopamine transmission has been one of the dominant neurobiological theories of schizophrenia for decades (27–31). However, a mechanistic, neural circuit-level link between dopamine and the symptoms of schizophrenia has remained a subject of speculation. Because striatal dopamine is well known to encode reward-related variables, particularly in ventral regions of the striatum (21), delusions and hallucinations have been suggested to arise from the misattribution of incentive salience mediated by aberrant reward prediction errors (28, 29) or, more broadly, precision-weighted prediction errors (32). Our finding that VS dopamine predicts HALIPs through reward expectations is consistent with these accounts. Because striatal dopamine also encodes perceptual variables such as perceptual confidence (33) and sensory stimulus intensity (23, 34)—particularly in the tail of the striatum (TS), which receives functionally relevant inputs from auditory cortex and thalamus (22, 35, 36)—it has further been suggested that hallucinations arise from a shift in perceptual detection threshold mediated by aberrant plasticity in thalamo-cortico-striatal loops (37). Our observations that TS dopamine is causally linked to HALIPs through perceptual expectations are broadly consistent with this account. TS also receives direct inputs from non-auditory sensory cortices and the multisensory intralaminar thalamus (38). This raises the possibility that TS dopamine not only may be critical for auditory HALIPs but also may play a role in HALIPs across other sensory modalities. Our model-inspired interpretation is that sustained elevations of dopamine modulate the integration of prior expectations and current sensory evidence (from cortical and thalamic inputs, respectively), thereby creating an imbalance that favors prior beliefs.

A limitation of our study is that it remains to be established whether HALIPs are produced by overlapping neural processes with spontaneous hallucinations and whether their quantitative measurement will be of clinical utility for psychotic disorders. Another limitation is that we did not investigate HALIPs in an

etiologically valid model of psychosis. Nonetheless, our findings offer insights into the relation between tonic dopamine and perception and provide a rigorous framework for generating testable propositions about the relationship between hallucinations and hallucination-like percepts, as well as their underlying neural circuits. Taken together, our cross-species computational psychiatry approach and results present a promising entry point to identify novel treatment targets in dopamine-dependent circuits and to develop urgently needed mechanistic treatments for schizophrenia.

REFERENCES AND NOTES

1. A. Carlsson, M. Lindqvist, Effect of Chlorpromazine or Haloperidol on Formation of 3-Methoxytyramine and Normetanephrine in Mouse Brain. *Acta Pharmacol. Toxicol.* **20**, 140–144 (1963). doi: [10.1111/j.1600-0773.1963.tb01730.x](https://doi.org/10.1111/j.1600-0773.1963.tb01730.x); pmid: [14060771](https://pubmed.ncbi.nlm.nih.gov/14060771/)
2. B. Angrist, G. Sathianathan, S. Wilk, S. Gershon, Amphetamine psychosis: Behavioral and biochemical aspects. *J. Psychiatr. Res.* **11**, 13–23 (1974). doi: [10.1016/0022-3956\(74\)90064-8](https://doi.org/10.1016/0022-3956(74)90064-8); pmid: [4461784](https://pubmed.ncbi.nlm.nih.gov/4461784/)
3. M. Laruelle, A. Abi-Dargham, Dopamine as the wind of the psychotic fire: New evidence from brain imaging studies. *J. Psychopharmacol.* **13**, 358–371 (1999). doi: [10.1177/026988119901300405](https://doi.org/10.1177/026988119901300405); pmid: [10667612](https://pubmed.ncbi.nlm.nih.gov/10667612/)
4. J. Reith et al., Elevated dopa decarboxylase activity in living brain of patients with psychosis. *Proc. Natl. Acad. Sci. U.S.A.* **91**, 11651–11654 (1994). doi: [10.1073/pnas.91.24.11651](https://doi.org/10.1073/pnas.91.24.11651); pmid: [7972118](https://pubmed.ncbi.nlm.nih.gov/7972118/)
5. O. D. Howes et al., The nature of dopamine dysfunction in schizophrenia and what this means for treatment. *Arch. Gen. Psychiatry* **69**, 776–786 (2012). doi: [10.1001/archgenpsychiatry.2012.169](https://doi.org/10.1001/archgenpsychiatry.2012.169); pmid: [22474070](https://pubmed.ncbi.nlm.nih.gov/22474070/)
6. N. R. Swerdlow, M. Weber, Y. Qu, G. A. Light, D. L. Braff, Realistic expectations of prepulse inhibition in translational models for schizophrenia research. *Psychopharmacology* **199**, 331–388 (2008). doi: [10.1007/s00213-008-1072-4](https://doi.org/10.1007/s00213-008-1072-4); pmid: [18568339](https://pubmed.ncbi.nlm.nih.gov/18568339/)
7. A. R. Powers, C. Mathys, P. R. Corlett, Pavlovian conditioning-induced hallucinations result from overweighting of perceptual priors. *Science* **357**, 596–600 (2017). doi: [10.1126/science.aan3458](https://doi.org/10.1126/science.aan3458); pmid: [28798131](https://pubmed.ncbi.nlm.nih.gov/28798131/)
8. C. M. Cassidy et al., A Perceptual Inference Mechanism for Hallucinations Linked to Striatal Dopamine. *Curr. Biol.* **28**, 503–514.e4 (2018). doi: [10.1016/j.cub.2017.12.059](https://doi.org/10.1016/j.cub.2017.12.059); pmid: [29398218](https://pubmed.ncbi.nlm.nih.gov/29398218/)
9. M. Carandini, A. K. Churchland, Probing perceptual decisions in rodents. *Nat. Neurosci.* **16**, 824–831 (2013). doi: [10.1038/nn.3410](https://doi.org/10.1038/nn.3410); pmid: [23799475](https://pubmed.ncbi.nlm.nih.gov/23799475/)
10. A. Kepecs, N. Uchida, H. A. Zariwala, Z. F. Mainen, Neural correlates, computation and behavioural impact of decision confidence. *Nature* **455**, 227–231 (2008). doi: [10.1038/nature07200](https://doi.org/10.1038/nature07200); pmid: [18690210](https://pubmed.ncbi.nlm.nih.gov/18690210/)
11. A. Lak et al., Orbitofrontal cortex is required for optimal waiting based on decision confidence. *Neuron* **84**, 190–201 (2014). doi: [10.1016/j.neuron.2014.08.039](https://doi.org/10.1016/j.neuron.2014.08.039); pmid: [25242219](https://pubmed.ncbi.nlm.nih.gov/25242219/)
12. P. Masset, T. Ott, A. Lak, J. Hirokawa, A. Kepecs, Behavior- and Modality-General Representation of Confidence in Orbitofrontal Cortex. *Cell* **182**, 112–126.e18 (2020). doi: [10.1016/j.cell.2020.05.022](https://doi.org/10.1016/j.cell.2020.05.022); pmid: [32504542](https://pubmed.ncbi.nlm.nih.gov/32504542/)
13. B. Hangya, J. I. Sanders, A. Kepecs, A Mathematical Framework for Statistical Decision Confidence. *Neural Comput.* **28**, 1840–1858 (2016). doi: [10.1162/NECO_a_00864](https://doi.org/10.1162/NECO_a_00864); pmid: [27391683](https://pubmed.ncbi.nlm.nih.gov/27391683/)
14. See supplementary materials.
15. P. R. Corlett et al., Hallucinations and Strong Priors. *Trends Cognit. Sci.* **23**, 114–127 (2019). doi: [10.1162/NECO_a_00864](https://doi.org/10.1162/NECO_a_00864); pmid: [27391683](https://pubmed.ncbi.nlm.nih.gov/27391683/)
16. J. H. Krystal et al., Subanesthetic effects of the noncompetitive NMDA antagonist, ketamine, in humans. Psychotomimetic, perceptual, cognitive, and neuroendocrine responses. *Arch. Gen. Psychiatry* **51**, 199–214 (1994). doi: [10.1001/archpsyc.1994.03950030035004](https://doi.org/10.1001/archpsyc.1994.03950030035004); pmid: [8122957](https://pubmed.ncbi.nlm.nih.gov/8122957/)
17. V. Bell, P. W. Halligan, H. D. Ellis, The Cardiff Anomalous Perceptions Scale (CAPS): A new validated measure of anomalous perceptual experience. *Schizophr. Bull.* **32**,

- 366–377 (2006). doi: [10.1093/schbul/sbj014](https://doi.org/10.1093/schbul/sbj014); pmid: [16237200](https://pubmed.ncbi.nlm.nih.gov/16237200/)
18. Pearson Symptom Checklist-90-Revised: www.pearsonclinical.com/psychology/products/100000645/symptom-checklist-90-revised-scl90r.html.
 19. J. van Os, R. J. Linscott, I. Myin-Germeys, P. Delespaul, L. Krabbendam, A systematic review and meta-analysis of the psychosis continuum: Evidence for a psychosis proneness-persistence-impairment model of psychotic disorder. *Psychol. Med.* **39**, 179–195 (2009). doi: [10.1017/S0033291708003814](https://doi.org/10.1017/S0033291708003814); pmid: [18606047](https://pubmed.ncbi.nlm.nih.gov/18606047/)
 20. A. Lak et al., Reinforcement biases subsequent perceptual decisions when confidence is low, a widespread behavioral phenomenon. *eLife* **9**, e49834 (2020). doi: [10.7554/eLife.49834](https://doi.org/10.7554/eLife.49834); pmid: [32286227](https://pubmed.ncbi.nlm.nih.gov/32286227/)
 21. W. Schultz, P. Dayan, P. R. Montague, A neural substrate of prediction and reward. *Science* **275**, 1593–1599 (1997). doi: [10.1126/science.275.5306.1593](https://doi.org/10.1126/science.275.5306.1593); pmid: [9054347](https://pubmed.ncbi.nlm.nih.gov/9054347/)
 22. Q. Xiong, P. Znamenskiy, A. M. Zador, Selective corticostriatal plasticity during acquisition of an auditory discrimination task. *Nature* **521**, 348–351 (2015). doi: [10.1038/nature14225](https://doi.org/10.1038/nature14225); pmid: [25731173](https://pubmed.ncbi.nlm.nih.gov/25731173/)
 23. W. Menegas, K. Akita, R. Amo, N. Uchida, M. Watabe-Uchida, Dopamine neurons projecting to the posterior striatum reinforce avoidance of threatening stimuli. *Nat. Neurosci.* **21**, 1421–1430 (2018). doi: [10.1038/s41593-018-0222-1](https://doi.org/10.1038/s41593-018-0222-1); pmid: [30177795](https://pubmed.ncbi.nlm.nih.gov/30177795/)
 24. F. Sun et al., A genetically-encoded fluorescent sensor enables rapid and specific detection of dopamine in flies, fish, and mice. *Cell* **174**, 481–496.e19 (2018). doi: [10.1016/j.cell.2018.06.042](https://doi.org/10.1016/j.cell.2018.06.042); pmid: [30007419](https://pubmed.ncbi.nlm.nih.gov/30007419/)
 25. T. Sigurdsson, K. L. Stark, M. Karayiorgou, J. A. Gogos, J. A. Gordon, Impaired hippocampal-prefrontal synchrony in a genetic mouse model of schizophrenia. *Nature* **464**, 763–767 (2010). doi: [10.1038/nature08855](https://doi.org/10.1038/nature08855); pmid: [20360742](https://pubmed.ncbi.nlm.nih.gov/20360742/)
 26. S. Parnaudeau et al., Inhibition of mediodorsal thalamus disrupts thalamofrontal connectivity and cognition. *Neuron* **77**, 1151–1162 (2013). doi: [10.1016/j.neuron.2013.01.038](https://doi.org/10.1016/j.neuron.2013.01.038); pmid: [23522049](https://pubmed.ncbi.nlm.nih.gov/23522049/)
 27. J. J. Weinstein et al., Pathway-Specific Dopamine Abnormalities in Schizophrenia. *Biol. Psychiatry* **81**, 31–42 (2017). doi: [10.1016/j.biopsych.2016.03.2104](https://doi.org/10.1016/j.biopsych.2016.03.2104); pmid: [27206569](https://pubmed.ncbi.nlm.nih.gov/27206569/)
 28. S. Kapur, Psychosis as a state of aberrant salience: A framework linking biology, phenomenology, and pharmacology in schizophrenia. *Am. J. Psychiatry* **160**, 13–23 (2003). doi: [10.1176/appi.ajp.160.1.13](https://doi.org/10.1176/appi.ajp.160.1.13); pmid: [12505794](https://pubmed.ncbi.nlm.nih.gov/12505794/)
 29. A. Heinz, Dopaminergic dysfunction in alcoholism and schizophrenia—Psychopathological and behavioral correlates. *Eur. Psychiatry* **17**, 9–16 (2002). doi: [10.1016/S0924-9338\(02\)00628-4](https://doi.org/10.1016/S0924-9338(02)00628-4); pmid: [11918987](https://pubmed.ncbi.nlm.nih.gov/11918987/)
 30. N. R. Swerdlow, G. F. Koob, Dopamine, schizophrenia, mania, and depression: Toward a unified hypothesis of corticostriatopallido-thalamic function. *Behav. Brain Sci.* **10**, 197–208 (1987). doi: [10.1017/S0140525X00047488](https://doi.org/10.1017/S0140525X00047488)
 31. D. R. Hemsley, J. N. P. Rawlins, J. Feldon, S. H. Jones, J. A. Gray, The neuropsychology of schizophrenia: Act 3. *Behav. Brain Sci.* **16**, 209–215 (1993). doi: [10.1017/S0140525X00029708](https://doi.org/10.1017/S0140525X00029708)
 32. R. A. Adams, K. E. Stephan, H. R. Brown, C. D. Frith, K. J. Friston, The computational anatomy of psychosis. *Front. Psychiatry* **4**, 47 (2013). doi: [10.3389/fpsyt.2013.00047](https://doi.org/10.3389/fpsyt.2013.00047); pmid: [23750138](https://pubmed.ncbi.nlm.nih.gov/23750138/)
 33. A. Lak, K. Nomoto, M. Keramati, M. Sakagami, A. Kepecs, Midbrain Dopamine Neurons Signal Belief in Choice Accuracy during a Perceptual Decision. *Curr. Biol.* **27**, 821–832 (2017). doi: [10.1016/j.cub.2017.02.026](https://doi.org/10.1016/j.cub.2017.02.026); pmid: [28285994](https://pubmed.ncbi.nlm.nih.gov/28285994/)
 34. W. Menegas, B. M. Babayan, N. Uchida, M. Watabe-Uchida, Opposite initialization to novel cues in dopamine signaling in ventral and posterior striatum in mice. *eLife* **6**, e21886 (2017). doi: [10.7554/eLife.21886](https://doi.org/10.7554/eLife.21886); pmid: [28054919](https://pubmed.ncbi.nlm.nih.gov/28054919/)
 35. N. D. Ponvert, S. Jaramillo, Auditory Thalamostriatal and Corticostriatal Pathways Convey Complementary Information about Sound Features. *J. Neurosci.* **39**, 271–280 (2019). doi: [10.1523/JNEUROSCI.1188-18.2018](https://doi.org/10.1523/JNEUROSCI.1188-18.2018); pmid: [30459227](https://pubmed.ncbi.nlm.nih.gov/30459227/)
 36. P. Znamenskiy, A. M. Zador, Corticostriatal neurons in auditory cortex drive decisions during auditory discrimination. *Nature* **497**, 482–485 (2013). doi: [10.1038/nature12077](https://doi.org/10.1038/nature12077); pmid: [23636333](https://pubmed.ncbi.nlm.nih.gov/23636333/)
 37. G. Horga, A. Abi-Dargham, An integrative framework for perceptual disturbances in psychosis. *Nat. Rev. Neurosci.* **20**, 763–778 (2019). doi: [10.1038/s41583-019-0234-1](https://doi.org/10.1038/s41583-019-0234-1); pmid: [31712782](https://pubmed.ncbi.nlm.nih.gov/31712782/)
 38. B. J. Hunsnutt et al., A comprehensive excitatory input map of the striatum reveals novel functional organization. *eLife* **5**, e19103 (2016). doi: [10.7554/eLife.19103](https://doi.org/10.7554/eLife.19103); pmid: [27892854](https://pubmed.ncbi.nlm.nih.gov/27892854/)

ACKNOWLEDGMENTS

We thank E. Bano, J. Constantino, P. Corlett, K. Hengen, G. Horga, T. Pinkhasov, S. Ryu, S. Ren, A. Kravitz, A. Shai, K. Yang, and C. Zorumski for discussions and comments on the manuscript, J. Kuhl for help with graphics, and L. Coddington for advice regarding our optogenetic stimulation protocol. **Funding:** Supported by Leopoldina–German Academy of Sciences fellowship LDPS 2010-03 (K.S.), German Research Foundation (DFG) grant OT 562/1-1 (T.O.), NARSAD Young Investigator grant 26726 (J.F.S.), and NIH grants MH097061 and DA038209 (A.K.). **Author contributions:** K.S. and A.K. conceived, designed, and interpreted the study. K.S. and M.B. collected the data. K.S., T.O., and J.F.S. analyzed the data. K.S., M.B., and A.K. wrote the manuscript. **Competing interests:** The authors declare no competing interests. **Data and materials availability:** All data are available in the main text or the supplementary materials.

SUPPLEMENTARY MATERIALS

science.sciencemag.org/content/372/6537/eabf4740/suppl/DC1
Materials and Methods
Figs. S1 to S12
Tables S1 and S2
Data S1
References (39–41)

28 October 2020; accepted 18 February 2021
[10.1126/science.abf4740](https://doi.org/10.1126/science.abf4740)